Int. J. Heat Mass Transfer. Vol. 30, No. 12, pp. 2583–2593, 1987
Printed in Great Britain

0017-9310/87 $3.00 + 0.00

On the modeling of turbulent evaporating sprays: Eulerian versus Lagrangian approach

A. A. MOSTAFA and H. C. MONGIA
Allison Gas Turbine Division, General Motors Corporation, Indianapolis, IN 46206, U.S.A.

(*Received* 29 *October* 1986 *and in final form* 29 *April* 1987)

Abstract—Recently developed mathematical models for turbulent evaporating sprays are described. The relative merits of Eulerian and Lagrangian approaches in handling the dispersed phase are discussed. These two approaches are evaluated vs reported data for evaporating dilute sprays (in the region $z/D \geq 50$), produced by an air-atomizing injector in a still environment. Results show that both approaches are successful in predicting the main features of this type of flow; however, the Eulerian approach performs better. The ignorance of the turbulence effects on the droplet motion is found to lead to significant errors when the mean relative velocity becomes comparable to the carrier phase r.m.s. velocity fluctuation. The one-size Eulerian treatment yields very comparable results to that of the multi-size treatment when the droplet size range is not very wide. Finally, the cost analysis for the two approaches demonstrates that the use of the Monte Carlo technique in simulating droplet dispersion is even more expensive than the multi-size Eulerian treatment.

1. INTRODUCTION

WORK IS currently being conducted in the area of mathematical modeling of the pertinent physicochemical processes occurring in turbulent reacting flows. This effort is needed to further improve current gas turbine combustor design methods [1] based on state-of-the-art models including turbulence, spray, and turbulence/chemistry interaction. This paper addresses one important aspect of combustion system analysis, the spray evaporation and dispersion modeling. The Lagrangian and Eulerian approaches for handling the liquid droplets are evaluated along with a recently developed turbulence model for two-phase flows [2].

In the Lagrangian approach, the evaporating spray is represented by a discrete droplet technique in which each computational droplet represents a number of similar physical droplets [3]. The computational droplets are treated by solving Lagrangian equations of mass, momentum, and energy with a prescribed set of initial conditions. The Monte Carlo sampling technique [4] is used to calculate spray properties including number density, droplet diameter, and mean and fluctuating droplet velocity components.

In the Eulerian approach, the evaporating spray is treated as an interacting and interpenetrating continuum [5, 6]. In this approach the governing equations for the two phases are similar to the Navier–Stokes equations with some extra source/sink terms. To use the Eulerian approach for the sprays, one must justify the continuum assumption for the dispersed phase as discussed by Batchelor [7] and Lumley [8]. For this assumption to be valid, each computational element must contain a large number of droplets so that statistically averaged properties can be assigned to the droplets. The droplet size should be sufficiently smaller than the Kolmogoroff microscale, η. Moreover, the interdroplet distance should be at least an order of magnitude smaller than η. Hinze [9] stated that the continuum assumption has proven to be applicable to situations that do not strictly meet this condition. Others (Crowe [10] and Soo [11]) showed that most practical systems involving gas particle mixtures satisfy the continuum assumption. The Eulerian approach to predict two-phase flows was employed by a number of researchers including Buckingham and Siekhaus [12], Pourahmadi and Humphrey [13], Rizk and Elghobashi [14], and Elghobashi *et al.* [15]. Similarly, the Lagrangian approach has been used by El-Banhawy and Whitelaw [16], Shuen *et al.* [17], El-Kotb *et al.* [18], and Boyson and Swithenbank [19].

Arguments persist among the researchers regarding the relative advantages and disadvantages of the Eulerian and Lagrangian approaches. The Eulerian approach can easily incorporate droplet diffusion effects since the randomness of the particulate phase is accounted for by way of the formulation. However, in the prediction of practical sprays, a prohibitively large number of finite difference grids are required to resolve the spray shape near the fuel nozzle. In this approach, the complex coupled partial differential equations of droplet motion need to be solved along with the gas phase equations in an iterative manner. The computational cost increases significantly with the increase of droplet-size groups that might be considered as distinctive phases. Finally, the continuum representation of the spray requires that the spray equations should be integrated throughout the domain even in the finite-difference cells that contain no droplets.

Unlike the Eulerian approach, the Lagrangian

NOMENCLATURE

B	transfer number, equation (13)
C	concentration of the vapor in the carrier phase
$c_\mu, c_{\varepsilon 1}, c_{\varepsilon 2}, c_{\varepsilon 3}$	coefficients in the turbulence model, equations (16) and (17)
C_D	drag coefficient, equations (7) and (8)
d	droplet diameter
D	nozzle diameter
F	interphase friction coefficient, equation (6)
g	gravitational acceleration
K	kinetic energy of turbulence
l_e	eddy size, equation (21)
$\dot{m}$	evaporation rate per droplet volume, equation (12)
m	droplet mass
N	number of droplets represented by the trajectory k
P	static pressure
r	distance in the radial direction
Re	Reynolds number, equation (9)
Sc	Schmidt number of the carrier phase
Sh	Sherwood number, equation (15)
t_i, t_0	the times when the droplet enters and leaves the carrier phase control volume
Δt	time the droplet takes to cross the carrier phase control volume
U	mean velocity of the carrier phase
u	fluctuating velocity of the carrier phase
$\mathbf{U}$	instantaneous velocity of the carrier phase
V	mean velocity of the droplets
$\mathbf{V}$	instantaneous velocity of the droplets
ΔV	control volume used in the carrier phase solution
v	fluctuating velocity of the droplets
z	distance in the axial direction.

Greek symbols

δ	molecular mass diffusivity of the vapor in air
ε	energy dissipation rate per unit volume
μ	dynamic viscosity of the carrier phase
ν_p	eddy viscosity of the droplets
ν_t	kinematic eddy viscosity of the carrier phase
ρ	material density
$\sigma_k, \sigma_\varepsilon$	coefficients in the turbulence model
σ_v	coefficient in the droplet's momentum equation
τ_d	droplet dynamic relaxation time, equation (19)
τ_e	turbulent eddy lifetime, equation (22)
τ_L	carrier phase Lagrangian time scale, equation (31)
τ_r	residence time of the droplet in the eddy, equation (23)
Φ	volume fraction, equation (5).

Subscripts

0	conditions at the nozzle exit
1	carrier phase
2	dispersed phase
c	conditions at the jet centerline
i	ith direction
L	conditions at the droplet surface
r	radial direction
z	axial direction.

Superscript

k	droplets in the size range k in the Eulerian formulation or the computational droplet of diameter d^k in the Lagrangian approach.

Abbreviations

DT	deterministic treatments
LDA	laser Doppler anemometer
LR	mass flow rate of the droplets compared with that of air at the nozzle exit
r.m.s.	root-mean-square of the velocity fluctuation
ST	stochastic treatments.

approach exhibits no numerical diffusion. However, the droplet dispersion must be incorporated through an empirical diffusion velocity or more expensive but accurate Monte Carlo methods [10]. In the stochastic or Monte Carlo method for calculating droplet trajectories, the instantaneous gas flow field must be modeled. Gosman and Ioannides [4] and Solomon *et al.* [20] split the isotropic turbulent gas field into two velocity components, mean (U_i) and fluctuation (u_i). During each droplet's flight u_i is randomly sampled and allowed to influence its motion. The cloud properties such as number density, average velocity, and temperature are obtained by averaging over a statistically significant sample of droplets.

The Monte Carlo method has the advantage of representing the direct effects of gas turbulence on droplet motion in a more realistic way. Shuen *et al.* [17] evaluated the Monte Carlo method for predicting the dispersed phase behavior by comparing the results with measurements of particle-laden jets. Their evaluation showed that this method provides good correlation with the data base. The Lagrangian approach requires interpolation between the finite difference meshes since the gas and droplet properties are

strongly coupled. Sirignano [21, 22] argued that the droplet properties should not be averaged over the numerical cell as suggested by Dukowicz [3] but rather a linear interpolation should be made.

In this paper, the governing equations using both the Eulerian and Lagrangian approaches for handling turbulent evaporating sprays are presented. The turbulence model for two-phase flows [22] is used for both approaches. In the Lagrangian treatment, the Monte Carlo method for simulating droplet dispersion is considered [4]. In the Eulerian treatment, the recent work of Mostafa and Elghobashi [6] on the droplet Schmidt number is adopted. The predictions are compared with the recent LDA spray measurements of Solomon *et al.* [20]. The results include distributions of the mean velocity, turbulence intensity and shear stress of the carrier phase, and the mean velocity of the droplets. Finally, a cost analysis of both Eulerian and Lagrangian approaches in predicting the considered data is made.

2. GOVERNING EQUATIONS

This section describes the assumptions and forms of the modeled equations to predict turbulent gaseous jet flows laden with vaporizing droplets using both the Eulerian and Lagrangian approaches for the spray and the Eulerian formulation for the carrier phase. The present study is restricted to the dilute spray regime where the droplet–droplet interaction is negligible. This implies that the droplets are sufficiently dispersed so that droplet collisions are infrequent. The initial breakup of liquid sprays or jets is not considered but the computations start away from the nozzle exit where individual droplets have formed. The droplets are assumed spherical as they undergo phase change. The mean flow is steady and isothermal and the material properties of the two phases are constant. Vaporization is assumed to be driven by the vapor concentration gradient.

In the Eulerian treatment, the continuous size distribution of the droplets is approximated by a finite number of size groups [23]. Each group is characterized by average quantities obtained from the solution of the conservation equations of mass and momentum.

The equations of the carrier phase and the droplets are coupled primarily by two mechanisms, mass and momentum exchange. The momentum exchange is due to both the aerodynamic forces exerted on the droplets and the momentum growth resulting from the relative velocity between the generated vapor and the surrounding gas [23]. The turbulent characteristics of the carrier phase are described by the two-equation turbulence model developed by Mostafa and Mongia [2]. The derivations of the governing equations are given by Mostafa and Elghobashi [6] and Mostafa and Mongia [2]. These equations, in the axisymmetric cylindrical form, are presented in the next section for application to a round jet flow.

2.1. *Carrier phase equations*

The mean continuity equation of the carrier phase is

$$\rho_1 U_{z,z} + \frac{\rho_1}{r}(rU_r)_{,r} = \sum_k \dot{m}^k. \tag{1}$$

The right-hand side of equation (1) represents the source term due to the droplet evaporation and the sink term in the continuity equation of the droplets (equation (26)).

In all governing equations, the comma-suffix notation indicates differentiation with respect to the spatial coordinates z or r.

The mean momentum equation of the carrier phase in the axial (z) direction is

$$\rho_1 U_z U_{z,z} + \rho_1 U_r U_{z,r} = -P_{,z} - \sum_k \Phi^k (F^k + \dot{m}^k)(U_z - V_z^k) + \frac{1}{r}(\rho_1 r \nu_t U_{z,r})_{,r}. \tag{2}$$

The mean momentum equation of the carrier phase in the radial (r) direction is

$$\rho_1 U_z U_{r,z} + \rho_1 U_r U_{r,r} = -P_{,r} - \sum_k \Phi^k (F^k + \dot{m}^k)(U_r - V_r^k) - \frac{2}{3}\frac{\rho_1}{r}(rK)_{,r}. \tag{3}$$

The kinematic eddy viscosity of the carrier phase is given by

$$\nu_t = c_\mu \frac{K^2}{\varepsilon}. \tag{4}$$

In the Eulerian approach, Φ^k is obtained from the solution of the continuity equation of the droplets in the group k while in the Lagrangian approach it is given by

$$\Phi^k = N\frac{\pi (d^k)^3}{6\Delta V}. \tag{5}$$

2.2. *The interphase friction factor F^k*

In the governing equations set, the drag force is expressed in terms of the interphase friction coefficient, F^k. In general F^k is given by

$$F^k = \frac{3\rho_1}{4d^k} C_D^k |\mathbf{U} - \mathbf{V}^k|. \tag{6}$$

Mostafa and Elghobashi [5] pointed out that the drag coefficient at low evaporation rates can be calculated from that of the standard experimental drag curve of a solid sphere with the same diameter. This curve is represented by [25]

$$C_D^k = (24/Re^k)(1 + 0.1315[Re^k]^{0.82 - 0.05w}), \quad 0.01 < Re^k \leqslant 20 \tag{7}$$

$$C_D^k = (24/Re^k)(1 + 0.1935[Re^k]^{0.6305}), \quad 20 < Re^k < 260 \tag{8}$$

where $w = \log_{10} Re^k$ and the droplet Reynolds number is based on the absolute value of the total instan-

taneous velocity

$$Re^k = \rho_1|\mathbf{U}-\mathbf{V}^k|d^k/\mu_1 \tag{9}$$

$$|\mathbf{U}| = \sqrt{\Sigma U_i^2} \tag{10}$$

$$|\mathbf{V}^k| = \sqrt{\Sigma (V_i^k)^2}. \tag{11}$$

2.3. *Mass transfer rate* m^k

The evaporation rate or the change rate of droplet diameter is determined by the physicochemical evaporative process and the condition of the turbulent surrounding flow. If changes in the droplet size and flow conditions occur slowly, the time derivatives in the differential equations governing the evaporation rate may be neglected and quasi-steady-state evaporation relations could be applied [6].

For quasi-steady-state evaporation of a spherical droplet suspended in a moving stream, the mass evaporated per unit time and unit droplet volume is

$$\dot{m}^k = \frac{12\delta\rho_1}{(d^k)^2}\ln(1+B)Sh^k. \tag{12}$$

When evaporation occurs due to the concentration gradient, the transfer number is given by

$$B = (C_L - C)/(1-C_L) \tag{13}$$

where C, C_L are the concentrations (defined as the ratio of the evaporated mass within a control volume to the mass of the carrier phase in the same volume) of the evaporating material at the free-stream conditions and at the droplet surface, respectively. C is obtained from the solution of the following modeled concentration transport equation:

$$\rho_1 U_z C_{,z} + \rho_1 U_r C_{,r} = \frac{1}{r}\left(\rho_1 r \frac{\nu_t}{\sigma_c} C_{,r}\right)_{,r} + \sum_k \Phi^k \dot{m}^k (1-C) \tag{14}$$

where σ_c is a coefficient of value 0.7 as given by Spalding [26].

The Sherwood number in equation (12) is given by the semiempirical formula of Ranz and Marshall [27] as follows:

$$Sh^k = \frac{\dot{m}^k}{\pi d^k \delta (C_L - C)} = 2 + 0.55 Re^{k\,1/2}\, Sc^{1/3} \tag{15}$$

where $Sc = \nu_1/\delta$ is the evaporated material Schmidt number.

2.4. *The turbulence model*

The turbulence kinetic energy equation (K) [2] is given by

$$\rho_1 U_z K_{,z} + \rho_1 U_r K_{,r} = \rho_1 \nu_t U_{z,r} U_{z,r} + \frac{1}{r}\left(\rho_1 \frac{\nu_t}{\sigma_k} r K_{,r}\right)_{,r} - \rho_1 \varepsilon - \sum_k 2K(F^k + \dot{m}^k)\Phi^k\left(1 - \frac{\tau_L}{\tau_L + \tau_d}\right). \tag{16}$$

The turbulence energy dissipation rate equation (ε) is given by [2]

$$\rho_1 U_z \varepsilon_{,z} + \rho_1 U_r \varepsilon_{,r} = C_{\varepsilon 1}\frac{\varepsilon}{K}[\rho_1 \nu_t U_{z,r} U_{z,r}] + \frac{1}{r}\left(\rho_1 \frac{\nu_t}{\sigma_\varepsilon} r \varepsilon_{,r}\right)_{,r} - c_{\varepsilon 2}\rho_1 \frac{\varepsilon^2}{K} - c_{\varepsilon 3}\frac{\varepsilon}{K} \times \sum_k \left[2K(F^k + \dot{m}^k)\Phi^k\left(1 - \frac{\tau_L}{\tau_L + \tau_d}\right)\right]. \tag{17}$$

The values of the coefficients appearing in equations (16) and (17) are listed in Table 1.

2.5. *Droplet equations: Lagrangian approach*

The equation of motion of each computational droplet, individually labeled by superscript k, in the ith direction is given by

$$\frac{d\mathbf{V}_i^k}{dt} = \frac{(\mathbf{U}_i - \mathbf{V}_i^k)}{\tau_d^k} + g_i \tag{18}$$

where

$$\tau_d^k = \frac{4d^k\rho_2}{3C_D^k\rho_1|\mathbf{U}-\mathbf{V}^k|}. \tag{19}$$

The instantaneous carrier phase velocity is given by

$$\mathbf{U}_i = U_i + u_i.$$

where U_i is determined from the solution of the mean flow equations of the carrier phase and u_i is chosen randomly from an isotropic Gaussian distribution with mean square deviation $(2/3)K$ where K is the turbulent kinetic energy of the carrier phase.

The droplet diameter in equation (18) is calculated from the solution of the mass transfer balance (equation (12)). The Reynolds number used in the solution of equations (12) and (18) is based on the instantaneous velocities for both the carrier phase and the droplets.

The droplet location at any instant of time is given by

$$\frac{dx_i^k}{dt} = \mathbf{V}_i^k. \tag{20}$$

For each droplet, after a turbulent correlation time (τ), a new value for u_i is chosen [4]. τ is the minimum of two time scales, one being a typical turbulent eddy lifetime (τ_e) and the other the residence time of the droplet in the eddy (τ_r). τ_e and τ_r are determined under the assumption that the characteristic size of the ran-

Table 1. Coefficients of the turbulence model

σ_k	c_μ	σ_ε	$c_{\varepsilon 1}$	$c_{\varepsilon 2}$	$c_{\varepsilon 3}$
1.0	$K-\varepsilon_1^{28}$	1.3	1.44	$K-\varepsilon_1^{28}$	2.0

domly sampled eddy is the dissipation length scale, l_e, while given by

$$l_e = c_\mu^{3/4} K^{3/2}/\varepsilon. \tag{21}$$

The eddy lifetime is then obtained as

$$\tau_e = l_e/|u_i|. \tag{22}$$

The residence time of the droplet in the eddy, that is, the time for a droplet to pass through that eddy, is estimated as

$$\tau_r = l_e/|\mathbf{U}-\mathbf{V}^k|. \tag{23}$$

Hence

$$\tau = \min(\tau_e, \tau_r). \tag{24}$$

The droplet equation of motion is integrated over as many interaction times as required for the droplet to traverse the required distance.

If a sufficiently large number of droplets is tracked in this way, the averaged behavior should represent the cloud and yield the effects of the turbulence of the carrier phase on the droplet motion.

2.6. *Droplet equations: Eulerian approach*

The momentum equation for droplets having an average diameter d^k in the kth diameter range in the axial (z) direction is [23]

$$\rho_2 \Phi^k V_z^k V_{z,z}^k + \rho_2 \Phi^k V_r^k V_{z,r}^k = -\Phi^k P_{,z} + F^k \Phi^k (U_z - V_z^k) + \frac{1}{r}(\Phi^k r \rho_2 \sigma_v v_p^k V_{z,r}^k)_{,r} + (\rho_2 - \rho_1) g \Phi^k. \tag{25}$$

The mean continuity equation of the kth group is written as

$$\rho_2 (\Phi^k V_z^k)_{,z} + \frac{\rho_2}{r}(r \Phi^k V_r^k)_{,r} - \rho_2 (v_p^k \Phi_{,z}^k)_{,z} - \frac{\rho_2}{r}(r v_p^k \Phi_{,r}^k)_{,r} = -\dot{m}^k \Phi^k. \tag{26}$$

The mean global continuity is

$$\Phi_1 + \sum_k \Phi^k = 1. \tag{27}$$

In equation (25) σ_v is a coefficient of value 0.7 as given by Melville and Bray [29].

2.7. *Turbulent diffusivity of liquid droplets*

The turbulent diffusivity of liquid droplets (ν_p^k) is evaluated by introducing the droplet Schmidt number σ_p^k defined as

$$\sigma_p^k = \frac{\nu_p^k}{\nu_t}. \tag{28}$$

Mostafa and Elghobashi [6] introduced an expression for calculating σ_p of particles having a constant drift velocity. At a dispersion time greater than the Lagrangian time scale of turbulence, this expression is given by

$$\sigma_p^k = (1 + 0.3[\mathbf{U}-\mathbf{V}^k]^2/[\overline{v^k}]^2)^{-1/2} \tag{29}$$

where the r.m.s. of the droplet velocity is given by

$$\frac{(\overline{v^k})^2}{u^2} = \frac{1}{1+\tau_d^k/\tau_L} \tag{30}$$

where

$$\tau_L = 0.35 K/\varepsilon. \tag{31}$$

The coefficient 0.3 in equation (29) was optimized based on the comparison of calculations of the lateral dispersion of solid particles and measurements of Snyder and Lumley [30] and Wells and Stock [31].

3. NUMERICAL SOLUTION

The governing equations of both the carrier phase and the droplets using the Eulerian approach are solved numerically using the marching finite-difference solution procedure developed and described in detail by Spalding [32, 33]. It was concluded that 35 cross-stream grid nodes yield grid-independent results.

In the Lagrangian approach, the ordinary differential equations governing droplet motion are solved using a second-order finite-difference algorithm. The total number of computational droplets was progressively increased until only 3% difference in the particle flow properties has accrued when using the optimized number and the next higher one. Accordingly, 4200 and 6000 computational droplets are used for the stochastic calculations of cases 1 and 2 while 280 droplets are computed when a comparison is made between the predictions of case 1 using the deterministic and stochastic methods.

The solution procedure and the boundary conditions are described in detail in refs. [2, 23] and will not be repeated here.

4. THE FLOW CONSIDERED

Solomon *et al.* [20] measured the carrier phase properties using a turbulent round jet with a laser Doppler anemometer (LDA), the droplet size and velocity using a shadow-photography technique, and the liquid mass flux with an inertial impaction method. An air-atomizing nozzle of 1.194 mm o.d. (D) was used to generate a Freon-11 spray. Detailed measurements were made on the two-phase jet with two loading ratios (LR) = 7.71 and 15.78. LR is defined as the mass flow rate of Freon-11 liquid at the nozzle exit to that of the nozzle air. The flow conditions for these two mass loadings will be referred to as cases 1 and 2, respectively.

Solomon *et al.* [20] measured the radial profiles of the mean and r.m.s. velocity, as well as the Reynolds stress at four stations, z/D = 50, 100, 250, and 500. The model calculations were started with the available measured profiles at z/D = 50. Mostafa [23] summarized the initial conditions needed for the com-

putation for the two loading ratios using the Eulerian approach. The initial turbulence dissipation rate (ε) profile is calculated from the measured turbulent shear stress and the axial velocity gradient. The initial volume fractions of the different groups (seven for case 1 and ten for case 2) are obtained from the measurements of the droplet mass flux, velocity distribution, and relative number density. The Freon vapor concentration profile C is obtained from the mixture fraction measurements and the state relations given by Solomon *et al.* [20].

The analysis of Solomon *et al.* showed that the droplet temperature at $z/D = 50$ is equal to Freon's saturation temperature, 240.3 K. In the present calculations it is assumed that the temperature of the carrier phase is equal to the surrounding air temperature (300 K) while the droplet surface temperature is 240.3 K. At these conditions, the density of the liquid Freon-11 is equal to 1518 kg m^{-3}, and the vapor concentration at the droplet surface is equal to 0.292. The carrier phase temperature profile measured at various axial stations ($250 \leqslant z/D \leqslant 500$) with a bare wire chromel–alumel thermocouple showed a maximum temperature difference of only 20°C. The evaporated mass is estimated [20] to be only 1.5–3% of the entrained air in cases 1 and 2, respectively. Therefore, constant properties are assumed for both phases in the present study.

5. RESULTS AND DISCUSSION

In this section, the predictions using the Eulerian and Lagrangian approaches are compared with the measured distributions of the mean axial velocities of the gas and droplets and the turbulence kinetic energy and shear stress of the gas. The computational efficiencies for handling the spray using the two approaches are compared for a loading ratio of 7.71.

Figure 1 shows the measured and predicted centerline axial velocity distribution of the carrier phase and those of the ten groups ($n = 1, 2, \ldots, 10$) for LR = 15.78. Here $n = 1$ ($n = k$ in the Eulerian approach) refers to the group that has the largest diameters, and $n = 10$ the smallest ones. It can be seen from this figure that the velocity difference between the carrier phase and the largest diameter group is greater than that of any other group. This behavior is attributed to the balance between the inertia of the droplet and the momentum exchange force. The inertia terms are proportional to $(d^k)^3$ [6] whereas the momentum exchange force is proportional to the droplet diameter with an exponent ranging from 1 to 1.7 depending on the droplet Reynolds number. By increasing the droplet size, the inertia becomes much greater than the momentum exchange forces; as a result the relative velocity between the droplets and the carrier phase ($U_z - V_z^k$) increases. This figure shows that the Eulerian approach performs better in correlating the droplet mean velocities than the Lagrangian approach.

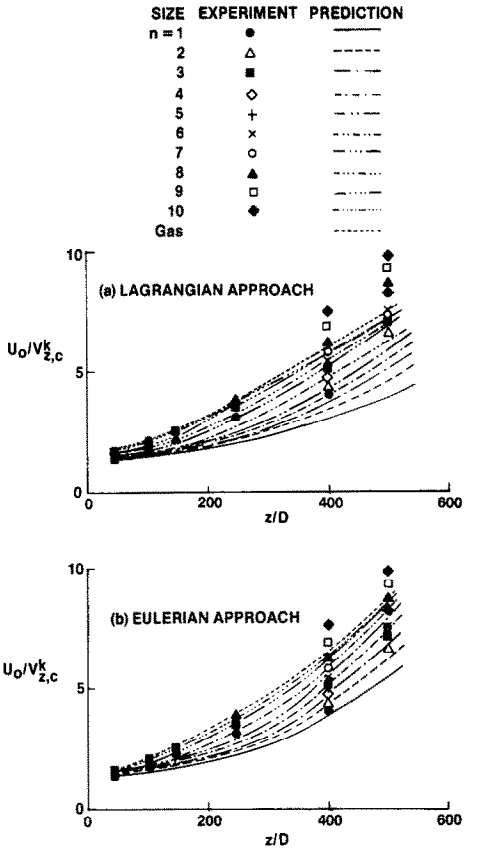

FIG. 1. Axial distribution of the mean centerline velocities.

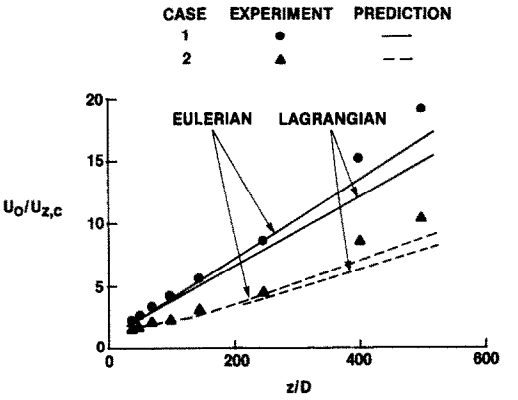

FIG. 2. Axial distribution of the gas mean centerline velocity.

Figure 2 shows the measured and predicted centerline distribution of the mean axial velocity of the carrier phase for the two mass loadings. It can be seen from this figure that the increase of the centerline velocity of the carrier phase compared with the single-phase value [34] is proportional to the mass loading ratio. This behavior is caused by the droplet mean momentum transfer and the effect of the droplets on the carrier phase turbulence quantities. Due to the carrier phase turbulence modulation caused by the droplets there is a reduction in the turbulent diffusion

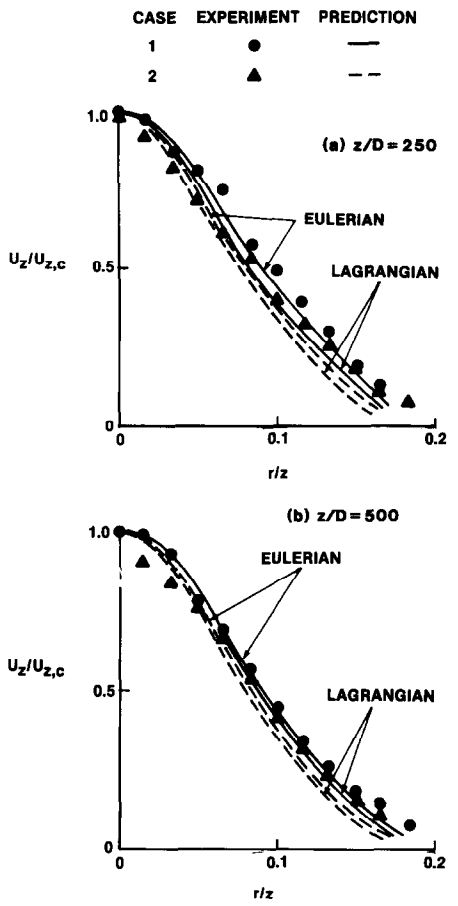

FIG. 3. Radial distribution of the gas mean axial velocities.

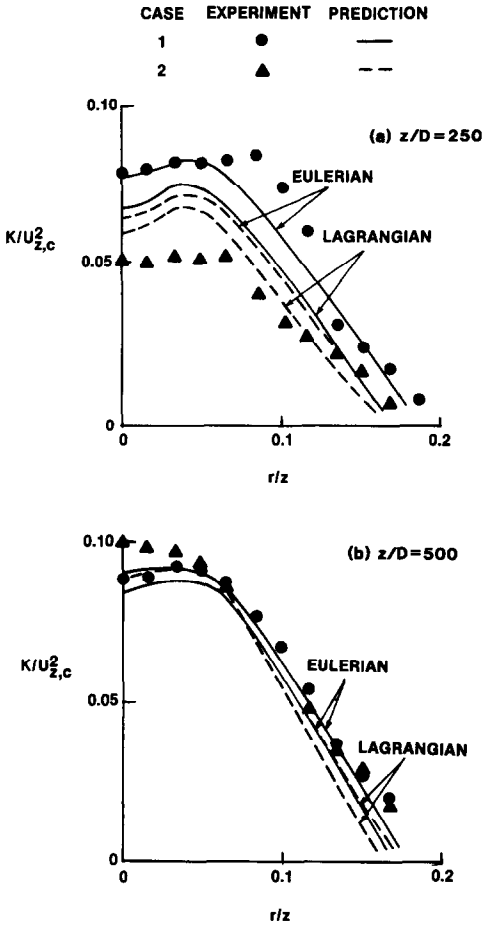

FIG. 4. Radial distribution of the gas kinetic energy of turbulence.

coefficient of the carrier phase compared with that of the single phase.

Figure 3 illustrates the radial profiles of the normalized mean axial velocities of the carrier phase at 250 and 500 nozzle diameters from the exit plane for both loadings. It can be seen from this figure that the jet width decreases with the increase of the mass loading ratio.

The influence of the loading ratio on the carrier phase turbulence energy and shear stress is presented in Figs. 4 and 5. The reduction in the turbulence energy or the increase in the dissipation rate of that energy is mainly caused by the turbulent correlation between the fluctuating relative velocity and that of the carrier phase. These two figures show that farther downstream from the nozzle exit the turbulence quantities asymptotically approach the single-phase jet values [34]. This is a consequence of the continuous diminution of the droplet volume fraction due to evaporation. Again it can be seen that the Eulerian approach gives better correlation with the data than the Lagrangian approach.

The predictions of the axial distribution of the Sauter mean diameter at the jet centerline compared with the experimental data are displayed in Fig. 6. Both approaches give good agreement with the data.

The superiority of the Eulerian approach in the present study over the Lagrangian approach is in agreement with the observations of many other previous workers as pointed out by Mostafa and Elghobashi [6] and Durst *et al.* [35]. This might be due to the fact that the Eulerian approach is conceptually more correct since the randomness of the dispersed phase is accounted for by way of the formulation.

It is noteworthy that the present observations are limited by the flow conditions of the data considered for comparisons and should be taken carefully for some other two-phase flow conditions. For instance, the parabolic nature of the flow minimized computer storage and numerical diffusion, both of which could be considered as drawbacks of the Eulerian approach.

In concluding this section, attention is drawn to the many advantages of the Lagrangian approach that we did not cover in the present study. As indicated by Sirignano [22], this approach is very useful when one is interested in resolution on a scale smaller than the average distance between droplets. It also poses no problems in handling the boundary conditions at a wall (rebounds or sticks) provided droplet rebound information is available [10]. Moreover, it is very appropriate to acquire more understanding and

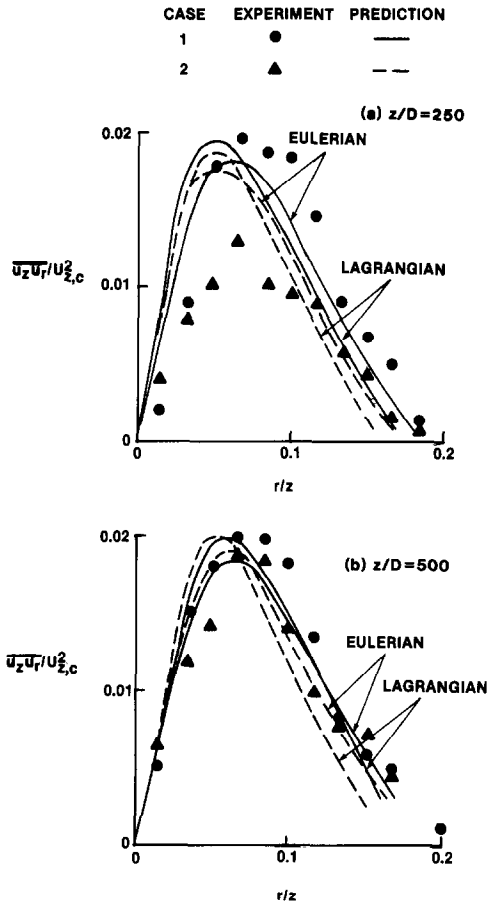

FIG. 5. Radial distribution of the gas shear stress.

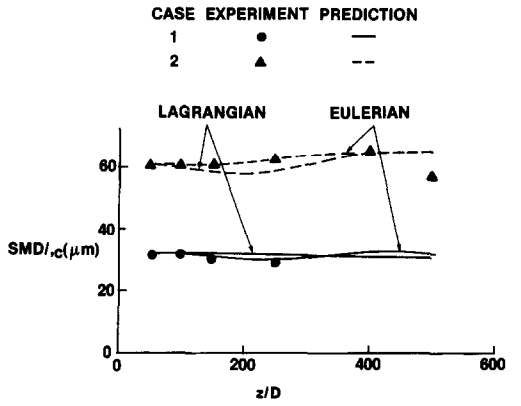

FIG. 6. Axial distribution of the Sauter mean diameter (SMD) along the jet centerline.

insights of the interaction between droplets and surrounding turbulent flow [36].

To afford three-dimensional gas turbine combustor calculations, many investigators have used the deterministic treatment instead of the more accurate stochastic treatment. In the deterministic treatment, the droplet dispersion due to gas turbulence is neglected and a significantly fewer number of trajectories is calculated. Similarly in the Eulerian approach, one could use a one-size formulation instead of the multi-size treatment.

Table 2 compares the carrier phase centerline mean axial velocity and kinetic energy of turbulence using the deterministic (DT) and stochastic treatments (ST). This table indicates a significant error in the predictions resulting from using DT in the modeling of the dispersed phase. The centerline mean velocity of the carrier phase becomes higher than the data by about 20%. This behavior could be attributed to completely ignoring the droplet dispersion in the DT which leads to more confinement of the droplets in the inner region of the jet. Due to this confinement and the higher inertial forces of the droplets, their centerline velocity decays with the downstream distance at a slower rate than that of the carrier phase (see Fig. 1). As a summary, ignoring the droplet dispersion leads to less spreading of the spray and higher momentum transfer to the carrier phase in the inner region of the jet.

It should be mentioned that the present findings of the importance of droplet dispersion in the modeling of turbulent two-phase flows have not been observed by Mostafa and Mongia [2]. This could be attributed to their flow conditions where the ratio between the relative mean velocity and the carrier phase r.m.s. velocity was very high. Mostafa and Elghobashi [6] pointed out that if this ratio is much greater than unity, the droplet will move from one eddy to another and the dispersion coefficient takes on an asymptotic form inversely proportional to the mean relative velocity. In such conditions, the droplet dispersion could be neglected and the DT might be used without significant errors. But due to the fact that the relative mean velocity diminishes with the downstream distance from the injector distance, the use of the DT in the modeling of turbulent evaporating sprays could lead to unrealistic results as demonstrated in Table 2.

Table 3 compares the centerline calculations using both one-size and multi-size (seven sizes) Eulerian treatments. The maximum difference due to the use of either treatment is 0.6 and 6% in the carrier phase mean velocity and kinetic energy of turbulence, respectively. This close agreement between the two treatments reflects that the effects of a spray of narrow size range similar to the considered case (17.5–52.5 μm) on the carrier phase could be simulated using average spray quantities. It is noteworthy that the one-size treatment gives only the global spray properties and not the detailed quantities which might be needed in many engineering applications. This explains the tendency of preferring the multi-size treatment in predicting two-phase flows over the one-size treatment.

A typical comparison between the different treatments for the spray in regard to machine time and memory requirements is presented in Table 4. This table shows that the stochastic treatment is expensive compared with other treatments. The cost of using the deterministic treatment with 280 trajectories is

Table 2. The effect of the deterministic (DT) and stochastic (ST) Lagrangian treatments on the predicted jet centerline values at LR = 7.71

Axial distance, z/D		100	200	300	400	500
$U_0/U_{z,c}$	DT	3.468	5.811	7.790	9.656	12.62
	ST	3.505	6.085	8.848	11.878	14.794
$K/U_{z,c}^2$	DT	0.0345	0.0519	0.0569	0.0619	0.0798
	ST	0.0342	0.0601	0.0727	0.0810	0.0849

Table 3. The effect of one-size (OS) and multi-size (MS) Eulerian treatments on the predicted jet centerline values at LR = 7.71

Axial distance, z/D		100	200	300	400	500
$U_0/U_{z,c}$	OS	3.580	6.555	9.862	13.190	16.496
	MS	3.580	6.502	9.802	13.163	16.496
$K/U_{z,c}^2$	OS	0.0371	0.0689	0.0825	0.0879	0.0898
	MS	0.0375	0.0677	0.0810	0.0873	0.0904

Table 4. IBM 3081 machine requirements using different spray approaches for predicting case 1 (LR = 7.71)

Approach	Eulerian		Lagrangian	
	One-size	Multi-size	Deterministic	Stochastic
Central memory storage (KB)	340	1388	304	1292
Central memory time (min)	0.37	1.721	0.444	4.423

quite comparable to the use of the one-size formulation in the Eulerian treatment.

6. CONCLUSION

Recent developments in the area of mathematical modeling of turbulent evaporating sprays are presented. The relative advantages and disadvantages of the two widely used approaches for handling spray dynamics, the Lagrangian and Eulerian approaches, are evaluated vs reported measurements. The results show that both approaches are able to predict the main features of a turbulent evaporating spray produced by an air-atomizing injector in a still environment; however, the Eulerian approach performs better in the considered region which is far from the nozzle exit; $z/D \geqslant 50$. The one-size Eulerian treatment yields very comparable results to that of the multi-size treatment if the droplet size range is not very wide. Ignoring turbulence effects on the droplet motion is found to lead to significant errors when the mean relative velocity becomes comparable to the r.m.s. velocity fluctuation of the carrier phase. Finally, the cost analysis for the two approaches shows that using the Monte Carlo technique in simulating droplet dispersion is even more expensive than the multi-size Eulerian treatment. This technique should be further investigated to obtain a balance between its high cost and potential improvements.

REFERENCES

1. H. C. Mongia and K. Smith, An empirical/analytical design methodology for gas turbine combustors, AIAA Paper No. 78-998 (1978).
2. A. A. Mostafa and H. C. Mongia, On the turbulence/particles interaction in turbulent two-phase flows, AIAA Paper No. 86-0215 (1986).
3. J. K. Dukowicz, A particle–fluid numerical model for liquid sprays, *J. Comput. Phys.* **35**, 229–253 (1980).
4. A. D. Gosman and E. Ioannides, Aspects of computer simulation of liquid fueled combustors, AIAA Paper No. 81-0323 (1981).
5. A. A. Mostafa and S. E. Elghobashi, A study of the motion of vaporizing droplets in a turbulent flow. In *Dynamics of Flames and Reactive Systems: Progress in Astronautics and Aeronautics* (Edited by J. R. Bowen, N. Monson, A. K. Oppenheim and R. I. Soloukhin), Vol. 95, p. 513. AIAA, New York (1984).
6. A. A. Mostafa and S. E. Elghobashi, Effect of liquid droplets on turbulence in a round gaseous jet, NASA CR-175063 (1986).
7. G. K. Batchelor, Transport properties of two-phase materials with random structure, *A. Rev. Fluid Mech.* **6**, 227–255 (1974).
8. J. L. Lumley, Two-phase and non-Newtonian flows. In *Turbulence* (Edited by P. Bradshaw), p. 289. Springer, Berlin (1978).
9. J. O. Hinze, Turbulent fluid and particle interaction. In

Progress in Heat and Mass Transfer, Vol. 6, p. 433. Pergamon Press, New York (1972).
10. C. T. Crowe, Review—numerical models for dilute gas–particle flows, *ASME J. Fluids Engng* **104,** 297–303 (1982).
11. S. L. Soo, *Fluid Dynamics of Multiphase Systems*. Blaisdell, Waltham (1967).
12. A. C. Buckingham and W. J. Siekhaus, Interaction of moderately dense particle concentrations in turbulent flow, AIAA Paper No. 81-0346 (1981).
13. F. Pourahmadi and J. A. C. Humphrey, Modeling solid–fluid turbulent flows with application to predicting erosive wear, *Int. J. Physicochem. Hydrodyn.* **4,** 191–219 (1983).
14. M. A. Rizk and S. E. Elghobashi, A two-equation turbulence model for two-phase dilute confined flows, *Int. J. Multiphase Flow* (1987), in press.
15. S. Elghobashi, T. Abou-Arab, M. Rizk and A. Mostafa, Prediction of the particle-laden jet with a two-equation turbulence model, *Int. J. Multiphase Flow* **10,** 697–710 (1984).
16. Y. El-Banhawy and J. H. Whitelaw, Calculation of the flow properties of a confined kerosene-spray flame, *AIAA J.* 1503–1510 (1980).
17. J. S. Shuen, A. S. P. Solomon, Q. F. Zhang and G. M. Faeth, A theoretical and experimental study of turbulent particle-laden jets, NASA CR-168293 (1983).
18. M. M. El-Kotb, O. M. F. Elbahar and M. M. Abou-Elail, Spray modeling in high turbulent swirling flow, Fourth Symposium on Turbulent Shear Flows, Federal Republic of Germany (1983).
19. F. Boyson and J. Swithenbank, Spray evaporation in recirculating flow, Seventeenth Symposium (International) on Combustion, The Combustion Institute, Pittsburg, Pennsylvania, pp. 443–453 (1979).
20. A. S. P. Solomon, J. S. Shuen, Q. F. Zhang and G. M. Faeth, A theoretical and experimental study of turbulent evaporating sprays, NASA CR 174760 (1984).
21. W. A. Sirignano, Fuel droplet vaporization and spray combustion theory, *Prog. Energy Combust. Sci.* **9,** 291–322 (1983).
22. W. A. Sirignano, The formulation of spray combustion models: resolution compared to droplet spacing, *J. Heat Transfer* **108,** 633–639 (1986).
23. A. A. Mostafa, A two-equation turbulence model for dilute vaporizing sprays, Ph.D. Thesis, University of California, Irvine (1986).
24. A. A. Mostafa and S. E. Elghobashi, A two-equation turbulence model for jet flows laden with vaporizing droplets, *Int. J. Multiphase Flow* **11,** 515–533 (1985).
25. R. Clift, J. R. Grace and M. E. Weber, *Bubbles, Drops, and Particles*. Academic Press, New York (1978).
26. D. B. Spalding, Concentration fluctuations in a round turbulent free jet, *Chem. Engng Sci.* **25,** 95–107 (1971).
27. W. F. Ranz and W. R. Marshall, Evaporation from drops, *Chem. Engng Prog.* **48,** 141, 173–180 (1952).
28. B. E. Launder, A Morse, W. Rodi and D. B. Spalding, The prediction of free shear flows a comparison of the performance of six turbulence models, Imperial College, TM/TN/19 (1975).
29. W. K. Melville and K. N. C. Bray, A model of the two-phase turbulent jet, *Int. J. Heat Mass Transfer* **22,** 647–656 (1979).
30. W. H. Snyder and J. L. Lumley, Some measurements of particle velocity autocorrelation functions in a turbulent flow, *J. Fluid Mech.* **48,** 41–71 (1971).
31. M. R. Wells and D. E. Stock, The effect of crossing trajectories on the dispersion of particles in a turbulent flow, *J. Fluid Mech.* **136,** 31–62 (1983).
32. D. B. Spalding, *GENMIX: a General Computer Program for Two-dimensional Parabolic Phenomena*. Pergamon Press, Oxford (1971).
33. D. B. Spalding, Numerical computation of multiphase flows, Lecture Notes, Thermal Sciences and Propulsion Center, Purdue University, West Lafayette, Indiana (1979).
34. A. J. Shearer, H. Tamura and G. M. Faeth, Evaluation of a locally homogeneous flow model of spray evaporation, *J. Energy* **3,** 271–278 (1979).
35. F. Durst, D. Milojevic and B. Schonung, Eulerian and Lagrangian predictions of particulate two-phase flows: a numerical study, *Appl. Math. Modelling* **8,** 101–115 (1984).
36. M. A. Rizk and S. E. Elghobashi, The motion of a spherical particle suspended in a turbulent flow near a plane wall, *Physics Fluids* **28,** 806–817 (1985).

SUR LA MODELISATION DES BROUILLARDS TURBULENTS EN EVAPORATION: APPROCHES EULERIENNE ET LAGRANGIENNE

Résumé—On décrit des modèles mathématiques récemment développés pour des brouillards turbulents qui s'évaporent. On discute les mérites respectifs des approches selon Euler et Lagrange pour traiter de la phase dispersée. Ces deux approches sont évaluées en liaison avec des données expérimentales pour des brouillards volatils diluées (dans la région $z/D \geqslant 50$), produits par un injecteur-atomiseur à air dans un environnement au repos. Les résultats montrent que les deux approches sont satisfaisantes pour prédire les configurations principales de ce type d'écoulement; néanmoins l'approche eulerienne est meilleure. L'ignorance des effets de la turbulence sur le mouvement des gouttelettes conduit à des erreurs significatives quand la vitesse relative moyenne devient comparable à la moyenne quadratique de la fluctuation de vitesse de la phase porteuse. Le traitement eulerien monodimensionnel conduit à des résultats très comparables à ceux du traitement multidimensionnel quand le domaine de taille de gouttelette n'est pas très étendu. Finalement, l'analyse du coût pour les deux approches montre que l'utilisation de la technique de Monte Carlo pour simuler la dispersion des gouttelettes est nettement plus onéreuse que le traitement eulerien multidimensionnel.

MODELLBILDUNG FÜR TURBULENTE, VERDAMPFENDE SPRÜHSTRÖMUNGEN: VERGLEICH ZWISCHEN EULER- UND LAGRANGE-ANSATZ

Zusammenfassung—Es wird über neue mathematische Modelle für turbulente, verdampfende Sprühströmungen berichtet. Die Vorzüge der Euler- und Lagrange-Ansätze bei der Berücksichtigung der zerstäubten Phase werden diskutiert. Diese zwei Ansätze werden ausgewertet und mit veröffentlichten Daten für verdampfende, verdünnte Sprühströmungen verglichen (für $z/D \geqslant 50$), die von einem Luftzerstäuber in einer ruhenden Umgebung erzeugt wurden. Die Ergebnisse zeigen, daß beide Ansätze zur Berechnung der Haupteigenschaften dieses Strömungstyps geeignet sind; der Euler-Ansatz hat jedoch Vorteile. Die Vernachlässigung der Turbulenzeffekte bei der Tropfenbewegung führt zu schwerwiegenden Fehlern, wenn die mittlere Relativ-Geschwindigkeit in derselben Größenordnung liegt wie der quadratische Mittelwert der Geschwindigkeitsschwankung der Trägersubstanz. Bei Berücksichtigung nur einer Tropfengröße liefert der Euler-Ansatz vergleichbare Ergebnisse gegenüber der Berücksichtigung mehrerer Tropfengrößen, wenn der Bereich der Tropfengröße nicht zu weit ist. Schließlich zeigt eine Kostenanalyse für die zwei Ansätze, daß die Monte-Carlo-Methode bei der Simulation der Tropfenzerstäubung noch kostenaufwendiger ist als der Euler-Ansatz mit der Berücksichtigung vieler Tropfengrößen.

ОТНОСИТЕЛЬНО МОДЕЛИРОВАНИЯ ТУРБУЛЕНТНЫХ ИСПАРЯЮЩИХСЯ СТРУЙ: СОПОСТАВЛЕНИЕ ОПИСАНИЙ ЛАГРАНЖА И ЭЙЛЕРА

Аннотация—Дано описание недавно предложенных математических моделей турбулентных испаряющихся струй. Проведено сопоставление формулировок Эйлера и Лагранжа, используемых для описания диспергирующей фазы. Выполнена оценка этих формулировок на основе имеющихся экспериментальных данных по испарению жидкостных струй (в области $z/D \geqslant 50$), распыляемых воздушной форсункой в неподвижную окружающую среду. Результаты показывают, что оба подхода позволяют успешно рассчитать основные характеристики этого вида течения, однако формулировка Эйлера является более результативной. Найдено, что пренебрежение влиянием турбулентности на лвижение капель приводит к существенным погрешностям в случае, когда знажение средней относительной скорости становится сопоставимой с ее среднеквадратичным значением. Результаты анализа, основанного на допущении Эйлера о наличии частиц одного размера, хорошо согласуются с результатами многоразмерного подхода, если диапазон размеров частиц не очень велик. И наконец, анализ стоимости расчетов этими методами показывает, что метод Монте-Карло, используемый для моделирования дисперсии капель, оказывается даже более дорогостоящим, чем многоразмерный метод Эйлера.